Thrust Effectiveness of Micronozzle

Evgeny I. SOKOLOV[*]

* Corresponding author: Tel.: +7 (911) 8373048; Fax: +7 (812) 5349513; Email: falcon_falcon@list.ru
State Polytechnic University, Saint – Petersburg, Russia

Abstract Thrust of the divergent part of axially symmetric micronozzle is under the study. It's input to total thrust is considered by means of analysis of relative thrust determined as divergent part's thrust related to nozzle's thrust without divergent part when gas issuing into vacuum. An inviscid one-dimensional flow is used as start condition of analysis. For this case, it is shown from conservation laws that divergent part of infinite length has finite relative thrust depending only on sort of issuing gas. Analysis of the influence of shear stress on thrust of divergent part with the use of theory of laminar boundary layer shows that optimal nozzle wall angle at the exit increases and optimal length decreases with decreasing of nozzle's dimension in comparison with initial inviscid case. This conclusion is approved by results of numerical simulation of flow inside nozzles with throat diameter 10 micrometers and various form of divergent part based on Navier – Stokes equations with both no-slip and slip wall conditions. Detailed analysis of flow shows advantage of micronozzles with wall form far from traditionally used in "large" thrusters.

Keywords: Conical nozzle, relative thrust, laminar boundary layer, Navier – Stokes equations, optimization

1. Introduction

Micronozzle as a part of propulsion system is the subject of interest during few last decades because of enlarging of development of small (micro- and nano-) satellites with total mass near 1 Kilogram and less.
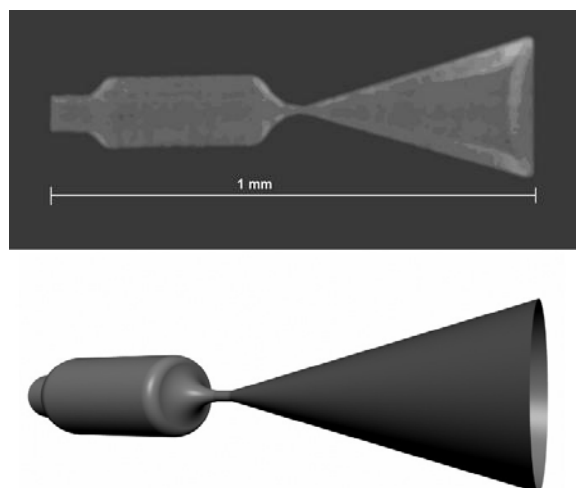

Fig. 1 Common view of microthruster

Their maneuverability may be realized by means of small thrusters with thrust less than 1 Newton. An example of microthruster (see at "Micropropulsion for small spacecraft", 2000) and it's 3D reconstruction which shows how conical nozzle looks like are placed on fig. 1

Basic parameters of conical nozzle are exit Mach number M_e, exit half – angle of nozzle divergence Θ_e, specific heat ratio of issuing gas γ and throat Reynolds number Re_*:

$$Re_* = \frac{\rho_0 U_* d_*}{\mu(T_0)} \qquad (1)$$

Here and then values marked with ($*$) are determined in the nozzle throat, ones marked with index (0) are taken at stagnation state, marked with lower (e) are determined at the nozzle's exit; ρ– density, U- velocity, d - diameter, μ - viscosity and T – temperature. It may be easily shown that $Re_* \sim p_0 d_*$. Let us assume for further study that the nozzle throat diameter is constant, equal, say, 10 micrometers. So, we will study only the input of divergent part of nozzle to total thrust in the case of issuing into vacuum when basic parameter Re_* decreases with decreasing of p_0. It is more convenient than changing of dimension because it does not require to build new grid with every new d_* during numerical

simulation (below, Pt 3)

When ideal gas issues from nozzle into vacuum (ambient pressure $p_\infty = 0$) flow in its divergent part is always supersonic. Some optimization methods of nozzle's wall form under various limitations have been developed about 50 years ago (sse, e.g., Miele, 1965). But, all of them based on taking into account only pressure distribution along the wall and neglecting of shear stress. This paper shows that with the decreasing of nozzle dimension negative input of shear stress to total thrust grows intensively, and mentioned above methods are invalid. Axially symmetric nozzles are under the study.

The following general expression is used for determination of total thrust of the nozzle in the case of $p_\infty = 0$ (Anderson, 2003):

$$F = \int_{S_e} (\rho U^2 + p)dS \qquad (2)$$

Here and then S – cross section's area

2. Inviscid One-Dimensional Flow

The start point of the study is the thrust of divergent part of nozzle in the case of inviscid perfect gas issuing into vacuum. With the use of well known relations for one – dimension isentropic flow (Anderson, 2003) one can obtain from (2):

$$F = \frac{\gamma+1}{2\gamma} Q a_* z(\lambda_e)\varphi_e \qquad (3)$$

Here λ- coefficient of velocity, φ_e – coefficient of thrust losses due to non – uniformity of the exit flow;

$$\lambda = \frac{U}{a_*} \quad , \quad \varphi_e = \cos^2\frac{\Theta_e}{2} \quad , \quad z = \lambda + \frac{1}{\lambda} \quad -$$

tabulated function, Q – exit flow rate.

In particular, for the nozzle without divergent part $\lambda_e = 1$, $z_e = 2$ and

$$F_* = \frac{\gamma+1}{\gamma} m a_* \qquad (4)$$

Let's relate thrust of divergent part of the nozzle to it's thrust without divergent part:

$$P = \frac{F - F_*}{F_*} = \frac{F}{F_*} - 1 \qquad (5)$$

With the use of (3) and (4) it is easy to obtain the following final expression of relative thrust P under the further study:

$$P = \left(\frac{z_e}{2} - 1\right)\cos^2\frac{\Theta_e}{2} \qquad (6)$$

It is useful to note that M and λ are tied with the following relation: $f_1(\lambda) = f_2(M)$;

$$f_1 = 1 - \frac{\gamma-1}{\gamma+1}\lambda^2, \quad f_2 = (1+\frac{\gamma-1}{2}M^2)^{-1}$$

In turn, non – dimensional exit cross area Σ is tabulated function of M or λ:

$$\Sigma = \left(\frac{r_e}{r_*}\right)^{-2} = q(M_e) = q'(\lambda_e), \quad \text{where}$$

$$q = \left(\frac{\gamma+1}{2}f_2\right)^{\frac{\gamma+1}{2(\gamma-1)}} M; q' = \left(\frac{\gamma+1}{2}f_1\right)^{\frac{1}{\gamma-1}}\lambda \quad (7)$$

It is visible from (7) that maximal exit Mach number $M_e = \infty$ corresponds to infinite Σ but to finite maximal λ and z values:

$$\lambda_m = \sqrt{\frac{\gamma+1}{\gamma-1}}, \quad z_m = \sqrt{\frac{\gamma+1}{\gamma-1}} + \sqrt{\frac{\gamma-1}{\gamma+1}} \quad (8)$$

With (6) and (8) it is easy to determine thrust P_m of divergent part of nozzle of infinite Σ and, evidently, infinite length. It's values for different gases are gathered in Table. 1.

In so far λ_m is finite, it is reasonable for further analysis to depict P as function of λ_e. Let's here and than take nitrogen ($\gamma = 1.4$) as basic gas with $\lambda_m = (6)^{0.5} \approx 2.449$. Thrust of supersonic part of conical nozzle with $\Theta_e = 10°$ and $\Theta_e = 20°$ as function of λ_e for $\gamma = 1.4$ is depicted on fig. 2 (broken curves). To determine P for nozzle of given form, one must determine λ_e from function q'(λ_e) with the use

of known r_* and r_e and than take P from curve on fig. 2. Some divergence of result on fig. 2 is only because of φ_e.

Table 1
Relative thrust of nozzle's divergent part of infinite length (ideal gas)

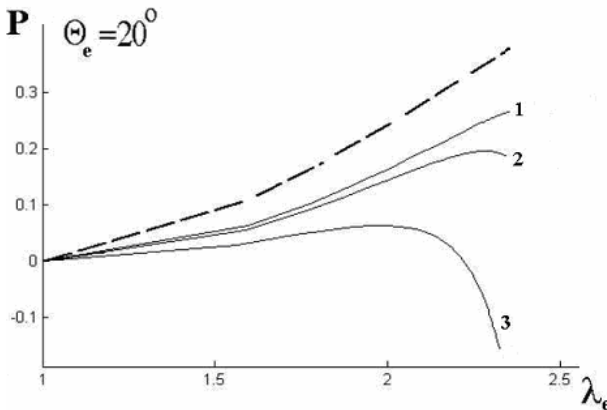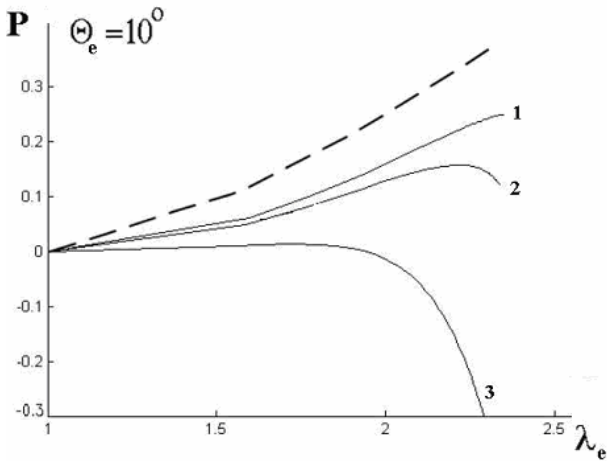| γ	1.67	1.4	1.25	1.13
P_m	0.2467	0.4256	0.6616	1.1387

Fig. 2 Relative thrust of nozzle's divergent part of infinite length. Broken curves - ideal gas, 1 - Re$_*$ = $1.23*10^5$, 2 - Re$_*$ = $1.23*10^4$, 3 - Re$_*$ = $1.23*10^3$

2. Viscous Flow

2.1 Laminar Boundary Layer

It is well known that in the case of finite but rather high Re$_*$ an influence of viscosity concentrates inside boundary layer (BL) originated along nozzle wall. The case of turbulent BL is outside our field of interest. The case of laminar BL is under the study.

Properties of nozzle flows in presence of developed laminar BL were studied intensively in connection with the development of hypersonic wind tunnels (Byrkin and Mezhirov ,1971). These results are used below.

Let's analyze an influence of BL upon the nozzle's thrust. Fig.3 illustrates schematically distribution of velocity at exit cross section; inviscid case corresponds to line 1. Real flow at this cross section may be divided into inviscid core and BL itself. The same distribution realizes at any cross section.
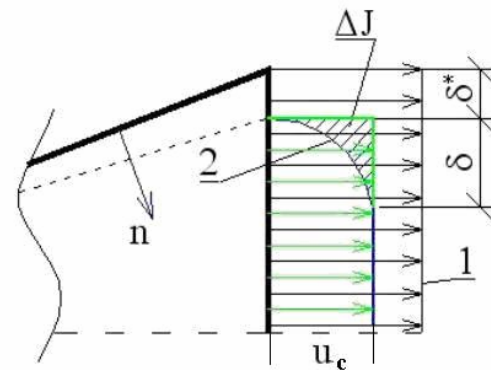

Fig. 3. Distribution of velocity at nozzle's exit. 1 – case of inviscid flow; 2 – 2 – flow, distributed by presence of boundary layer

Decreasing of velocity inside BL to zero on the wall realizes in decreasing of flow rate. This effect is described with the help of so-called "displacement thickness" δ^* (Shlihting, et al, 2004). For its calculation, the following expression is used (Byrkin and Mezhirov, 1971):

$$\frac{\delta^*}{r_*} = \frac{F_1(T_w)F_2(M)\sqrt{X}}{\sqrt{\sqrt{\frac{\gamma+1}{\gamma-1}} \text{Re}_*}} \qquad (9)$$

Here $F_1(T_w) = \left(\frac{T_0}{T_w}\right)$ - function of relative nozzle wall temperature, $X = \frac{x}{r_*}$ - relative distance between throat and cross section under consideration and $F_2(M) = 1.36M^2 - 1.1M - 0.026$ - function of core Mach number.

So, for taking into account decreasing of flow rate wall at any cross section of the nozzle must be replaced inside on value δ^* (9) in n direction (fig.3). Cross section obtains smaller radius and real Mach number in inviscid core M_c which must be recalculated with (7) will be evidently lower than initial (vectors U_c on fig.3). This new Mach Number M_c have to be placed again into (9) for recalculation of δ^*. This procedure of δ^* and M_c determination suggested by Byrkin and Mezhirov (1971) usually converges in 3 – 4 iterations. Then, final velocity distribution must take into account no-slip wall condition which originate BL of thickness δ (line 2, fig.3). As result, difference between inviscid and viscous velocity inside BL will lead to the defect of momentum ΔJ (fig.3):

$$\Delta J = \int_S (\rho_c U_c^2 - \rho U^2)dS$$

Relative thrust of supersonic part of the nozzle with wall BL is then calculated as follows:

$$P = \left(\frac{z_e}{2} - 1\right)\cos^2\frac{\Theta_e}{2} - \frac{\Delta J}{F_*} \qquad (10)$$

In turn, ΔJ may be expressed with the help of conventional BL thicknesses (Shlihting, et al, 2004), which finally gives:

$$\Delta J = 2\pi\rho_c U_c^2 r\delta^*\left(1 + \frac{\theta}{\delta^*}\right) \qquad (11)$$

Here θ - momentum thickness. Let's approximately assume Pr =1 and describe velocity profile across laminar BL as cubic parabola (Shlihting, et al, 2004). It allows, through some intermediate transformations, to obtain:

$$\frac{\delta^*}{\theta} = 2.69 F_1(T_w)F_2^{-1}(M) + \frac{\gamma - 1}{2}M^2 \qquad (12)$$

Finally, the following procedure of calculation of function $P(\lambda)$ along the divergent part of conical nozzle of given form is suggested:

i)   for taken number of cross sections of conical nozzle under consideration, Mach number M and coefficient of velocity λ of inviscid flow are calculated with (7);

ii)   displacement thickness δ^* and core Mach number M_c are calculated then for any cross section in iteration procedure with (7) and (9);

iii) for each core Mach number M_c value ΔJ is determined with the help of (11), (12). It allows to calculate required function P with (10).

Results of this procedure are placed on fig. 2 (curves 1÷3 for $Re_* = 123000$, 12300 and 1230 respectively). Each nozzle has following parameters: $\lambda_e = \lambda_m - 0.05 = 2.4$; $M_e = 10.5$; $d_e = 90.9d_*$; 25 cross sections with uniform x distribution along nozzle are taken for calculation. In the case of $Re_* \sim 10^6$ decreasing of P is monotonic (curves 1), but for medium $Re_* \sim 10^5$ maximum of P appears for both nozzles (curves 2).

For obtaining more deep understanding of result let's look at common condition of thrust maximization. Thrust is an integral of x – component of sum of normal and tangential stresses at current point A of nozzle wall (fig. 4):

$$F = \int_{s_w} (p\sin\Theta - \tau\cos\Theta)dS_w =$$
$$= 2\pi\int_r r(p - \tau\cot\Theta)dr \qquad (13)$$

Here p and τ are normal and tangential (shear) stresses. For nozzle of conventional size input of τ is negligibly small. Second item in (13) does not include in procedure of wall's form optimization (Miele, 1962). With decreasing of Re_* p and τ become compatible and negative input of shear stress to F grows intensively, particular for small Θ. That's why nozzle with $\Theta_e = 20°$ is more effective for smallest calculated Re_*. This conclusion confirms expressively when P is depicted as function of X for nozzle of given $\Sigma = 200$ (fig. 5). These results clearly show advantage of nozzle of larger Θ_e at low Re_*.
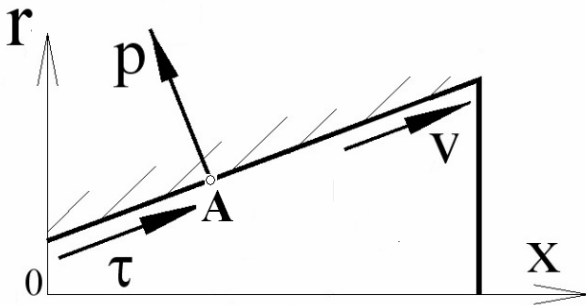
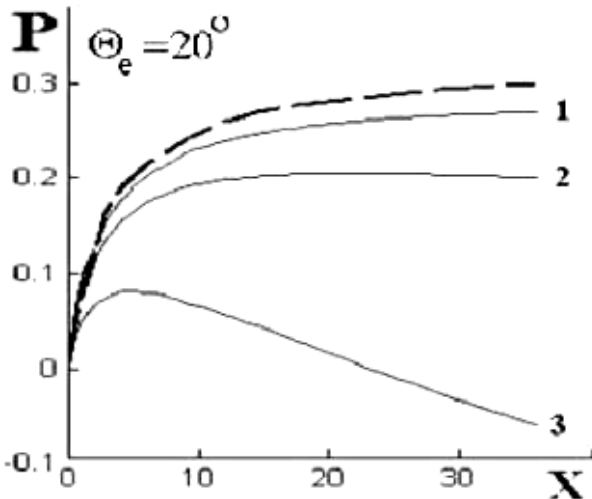Fig. 4. Stresses, acting on nozzle's wall at some point A

Fig. 5. Relative thrust of nozzle's divergent part, $\Sigma =$ 200. Notes are the same as on fig. 2

2.2 Simulation with Navier – Stokes Equations

Let's consider results of numerical modeling of flow under the study with the use of exact transient Navier – Stokes equations. Program package VICON developed for "Laser Systems Ltd" (St. Petersburg, Russia) is used for it. Final steady flow is reached as result of stabilization in time. Algorithm is based on principle of splitting of physical processes: inviscid part is calculated by 2nd order ENO scheme (Yang and Hsu,1992), viscous components – by procedure of Ignatiev (1995). Both no-slip and slip boundary conditions are possible on walls as well as T=T_w or temperature jump. After stabilization in time, integral (2) is calculated numerically. VICON had been verified and validated in wide range of simulations of gasdynamic processes in chemical lasers (see, e.g., Boreysho et al., 2005).

Initial flow geometry under calculation (nozzle 1) is shown on fig. 6. Nozzle parameters are the following: $M_e = 6$ ($\lambda_e = 2.29$),

$\Theta_e = 15°$, issuing gas – N_2, $p_0 = 2*10^6$Pa, $T_0 =$ 1500K, $T_w = 300$K, $Re_* = 1230$. Region is covered by regular grid, about 100 cells are placed across exit, total number of sells is about 10^6. Gas comes into the divergent part of nozzle through cross section 1 with parameters correspond to M =1.02; ambient parameters right of cross section 2 (nozzle exit) are following: $p_\infty = 10$Pa, $T_\infty = 1500$K. Relative thrust P is determined by (5); required values F and F_* are caculated as integrals (2) at cross sections 1 and 2. Calculated relative thrust at this regime P = - 0.788. This value is much more lower than depicted on figs. 2, 3 for $\lambda_e =$ 2.29. The reason of it is following: named results were obtained with the use of model of laminar boundary layer. More exact model used here shows totally viscous flow (gray U_x diagram on fig. 6). That's why this nozzle produces drag not thrust.
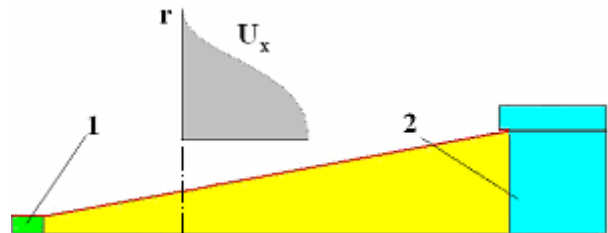

Fig. 6. Flow pattern of nozzle 1($M_e = 6$, $\Theta_e = 15°$)
1 – throat; 2 - ambient space

In accordance with recommendations proclaimed above let's cut nozzle under calculation up to 1/3 of initial length (nozzle 2: M_e = 2.59, $\lambda_e = 1.854$). As one can see from fig. 7, such configuration has bottom flat surface with diameter equal to exit diameter of initial nozzle and orthogonal to axis. Bottom pressure is included into (2) for calculation of total x-force. It allowed to obtain relative thrust P = 0.286 — value higher than depicted on figs. 2, 3 for $\lambda_e = 1.854$ in the contrary with previous case. Distribution of Mach Number on fig. 7 shows origination of subsonic boundary layer in radially spreading bottom flow.

In order to increase an input of bottom pressure into total thrust, radial spreading along bottom surface is stopped by addition of cylindrical coaxial wall. It's length was taken
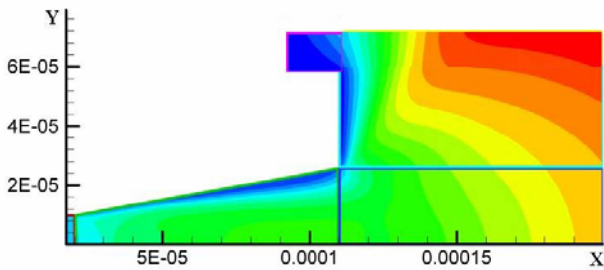
arbitrarily and equals to bottom radius.

Fig. 7. Mach Number distribution of nozzle and plume flow for nozzle 2 (M_e = 2.59, Θ_e = 15°)

(nozzle 3, fig. 8). Calculated distribution of Mach number is visible there, too. In comparison with fig 7 one can see here a large region of subsonic speed in the corner near horizontal cylindrical wall. This effect leads to growing of pressure and, finally, growing of thrust: P = 0.389. More explicitly it is seen in comparison of distribution of bottom pressure for these two nozzles (fig. 9, curves numbered according nozzles).
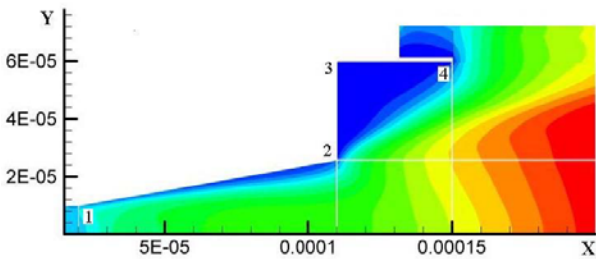

Fig. 8. Mach Number distribution of nozzle and plume flow for nozzle 3 (M_e = 2.59, Θ_e = 15°)

It have to be noted that the same calculations were done with slip wall boundary condition. Coefficient of accommodation C = 0.7 did not affect visibly upon results. With C = 0.1 BL disappeared and P increased but such coefficient seems unreal.

3. Conclusions

In spite of approximate feature, theory of laminar boundary layer gives real qualitative description of effects originated due to decreasing of nozzle's dimension. Growing of negative input of shear stress to total X – force (13) has to be included into procedure of optimization of micronozzles. It was effectively shown on nozzle 3 for which notable growth

of P was reached by addition of "corner" to the form of traditional divergent part. Presented above numerical results were obtained when corner points of this nozzle (1 - 4, fig.8) were put to its positions very arbitrarily. Their relative replacement is the subject of optimization. For instance, according to (13) making distance between points 3 and 4
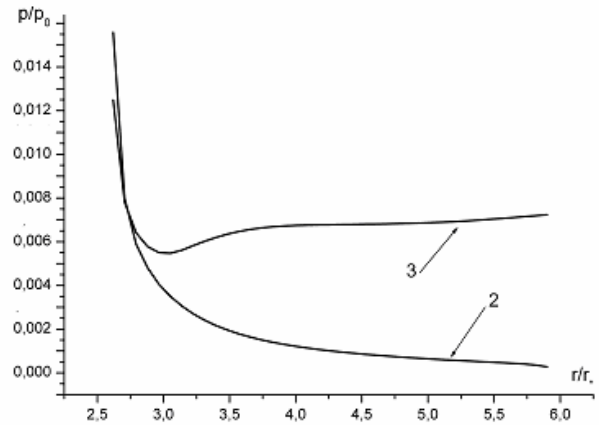

Fig. 9. Pressure distribution along bottom surface for nozzles 2 and 3

shorter decreases input of τ into total force; smaller radius of point 3, maybe, will increase bottom pressure and P as result; lines 2-3 and 3-4 may have another angles, and so on.

Results described here are in a good accordance with other ones obtained in studies of flows in micronozzles. So, numerical simulation of flow in micronozzles done by Louisos W.F. and Hitt D. L., (2008) with the use of Navier –Stokes equations (Re* =15 – 800, Θ_e =10° – 50°) shows that maximum of thrust grows with length decreasing and realizes at Θ_e = 30°. With this angle, growing of thrust compensates with non – uniformity loses described by factor φ_e in (3). The same qualitative conclusions were done by Ketsdever A.D., et al., (2005) with the use of Direct Simulation Monte – Carlo solver for simulation of rarefied micronozzle flow.

References

Anderson, J., 2007. Fundamentals of Aerodynamics. McGraw-Hill Co. Boston

Boreysho, A.S., Vasiliev, D.N., Evdokimov, I.M., Morozov, A.V., Savin, A.V., 2005. Medium Range COIL: towards Realization. AIAA Paper 2005-5169

Byrkin, A.P., and Mezhirov, I. I., 1971. On Calculation of Gas Flow in Hypersonic Nozzle with Account of the Influence of Viscosity. TsAGI Scientific Notes, 6, 105 - 113 (in Russian)

Ignatiev, A.A., 1995. Finite Difference Scheme for Viscous Part of Navier – Stokes Equations. Mathematical Modeling, 8, 107 – 116 (in Russian)

Ketsdever A.D., Clabough M.T., Gimelshtein S.F., Alexeenko A.A., 2005. Experimental and Numerical Determination of Micropropulsion Device Efficiencies at Low Reynolds Numbers. AIAA J, 43, 633 - 641

Louisos W.F., Hitt D.L., 2008. Viscous Effects on Performance of Two-Dimensional Supersonic Linear Micronozzles. Journal of Spacecraft and Rockets 45, 706 – 715

Micropropulsion for Small Spacecraft, 2000. (edited by Micci M. M., Ketsdever A. D.). Progress in Astronautics and Aeronautics, Vol. 187. AIAA, Reston, VA

Miele A., 1965. Theory of Optimum Aerodynamic Shapes. Academic Press, N.-Y.

Shlihting, G., Gersten, K., Krause, E., Oertel, H., Mayes, C., 2004. Boundary-Layer Theory. Springer, N.-Y.

Yang, J.Y., and Hsu, C.A, 1992. High-Resolution, Nonoscillatory Schemes for Unsteady Compressible Flows. AIAA J., 30, 1570-1575